Advances and Applications in Mechanical Engineering and Technology
Volume 1, Number 1, 2010, Pages 1-17

COMPLIANCE MODEL FOLLOWING FORCE CONTROL FOR OPEN-ARCHITECTURAL INDUSTRIAL ROBOTS

FUSAOMI NAGATA[1], TAKANORI MIZOBUCHI[1] and KEIGO WATANABE[2]

[1]Tokyo University of Science
Yamaguchi, 1-1-1 Daigaku-Dori
Sanyo-Onoda 756-0884
Japan
e-mail: nagata@ed.yama.tus.ac.jp

[2]Okayama University
3-1-1 Tsushima-naka
Kita-ku, Okayama 700-8530
Japan

Abstract

This paper presents a compliance model following force control that can take account of a desired position in the force control, and gives a transformation technique from the position command to the torque command in order to apply the controller to an industrial robot, whose servo system is technically opened, or to implement it in computer simulations. Next, to determine a suitable compliance without trial and error, a method that produces desired time-varying damping for critical damping is introduced by using the information on inertia and Jacobian. Simulation results using a dynamic model of an industrial robot PUMA560 have shown that the proposed methods are effective for realizing the controller in the robot, and for improving the force control performance.

Keywords and phrases: mechatronics and robotics, compliance, impedance control, force control, critically damped response, PUMA560, MATLAB.

Received November 14, 2009

1. Introduction

Industrial robots have been remarkably progressed, and they have been applied to many tasks, such as painting, welding, sealing, handling, and so on. In these cases, it is important to control the position of the end-effector precisely, and the force control is not necessary. However, if the robots are applied to grinding and polishing works, it is necessary to use a compliant force control just like being done by humans [6]. Two representative methods on the force control have been ever proposed. The one is a hybrid position/force control method [7], which controls the contact force itself to an object. And the other is an impedance control method [4], which controls the contact impedance parameters such as inertia, damping, and stiffness. The hybrid position/force control method and impedance control method are suitable for profiling motion along objects, and for the task, which needs compliant motions, respectively. However, to the best of the author's knowledge, force control methods have not been successfully applied to industrial robot applications in actual industrial fields so many yet.

Recently, hybrid compliance/force control (HCC) [5] were proposed and have received much attention to apply them to robots. In this method, a position control, a compliance control, and a force control can be switched for each direction in Cartesian space. In addition, two kinds of command approaches depending on the torque or position information are provided. When applying the HCC method to an industrial robot, it is required to adjust the suitable compliance for each task. However, a systematic adjustment method has not been successfully established. In the conventional HCC, the desired compliance is determined by repeating many simulations, or by trial and error. So, it is necessary to develop a practical approach, which can calculate the suitable compliance in a short time. Also, as for the position-based HCC, a solution of the desired differential equation is shown, however, it is not clear on how to simulate the position-based HCC, (i.e., how to yield joint driving torques) and how to apply it to an actual industrial robot.

To determine the suitable compliance, this paper proposes an effective method, which varies a desired damping to be in contact with an object at the critical damping [3], according to the inertia and Jacobian of manipulator changing nonlinearly. This method can systematically generate the desired damping for keeping in contact with an object suppressing undesirable oscillations and overshoots. We further propose a position-based compliance model following force control method (CMFFC), in which a desired position is given in the force control. An explanation on how to apply the method to an industrial robot is described in detail. Simulation results using a dynamic model of an industrial robot PUMA560 have shown that the position-based CMFFC, using a technically opened inner servo system is effective for simply realizing a force controller, and the tuning method of desired damping considering the critical damping can improve the force control performance. Figure 1 shows a photo of KAWASAKI JS10, which is one of PUMA560 type industrial robots.

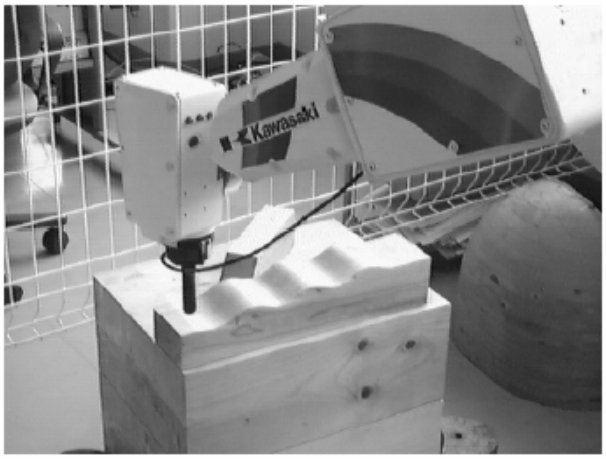

Figure 1. PUMA560 type industrial manipulator.

2. Compliance Model Following Force Control

2.1. Proposition of compliance model following force control

First of all, a desired impedance equation of a robot manipulator with 6 degree-of-freedom is designed in Cartesian space, which can be represented by

$$\boldsymbol{M}_x(\theta)\ddot{\boldsymbol{x}} + \boldsymbol{B}_d(\dot{\boldsymbol{x}} - \dot{\boldsymbol{x}}_d) + \boldsymbol{K}_d(\boldsymbol{x} - \boldsymbol{x}_d) = \boldsymbol{SF} + (\boldsymbol{I} - \boldsymbol{S})\boldsymbol{K}_f(\boldsymbol{F} - \boldsymbol{F}_d), \quad (1)$$

where $\boldsymbol{x}$, $\dot{\boldsymbol{x}}$, $\ddot{\boldsymbol{x}}$ are the position, velocity, and acceleration vector, respectively. $\boldsymbol{M}_x(\theta)$ is the actual inertia matrix, $\boldsymbol{F}$ is the force and moment vectors acting on the end-effector, $\boldsymbol{K}_f$ is the force feedback gain matrix. $\boldsymbol{x}_d$, $\dot{\boldsymbol{x}}_d$, and $\boldsymbol{F}_d$ are the desired position, velocity, and force/moment vectors; $\boldsymbol{B}_d$ and $\boldsymbol{K}_d$ are the coefficient matrices of desired damping and stiffness, respectively. $\boldsymbol{S}$ and $\boldsymbol{I}$ are the diagonal switch matrix and identity matrix, respectively. It is assumed that $\boldsymbol{K}_f$, $\boldsymbol{B}_d$, and $\boldsymbol{K}_d$ are positive-definite diagonal matrices. It should be noted that Equation (1) has no switch matrix $\boldsymbol{S}$ applied to the desired stiffness in HCC. We consider here a position control strategy in the direction of force control, because that, if the object dynamics is known, the response is improved by using the desired position information. Of course, if the measured position is substituted into the desired position, the effect of stiffness term will be excluded. Note that Equation (1) becomes a compliance control system in all directions in case of $\boldsymbol{S} = \boldsymbol{I}$, whereas, it becomes a force control system in all directions in case of $\boldsymbol{S} = \boldsymbol{0}$.

Generally, the dynamic model of a manipulator in Cartesian coordinate system is given by

$$\boldsymbol{M}_x(\boldsymbol{\theta})\ddot{\boldsymbol{x}} + \boldsymbol{H}_x(\boldsymbol{\theta}, \dot{\boldsymbol{\theta}}) + \boldsymbol{G}_x(\boldsymbol{\theta}) = \boldsymbol{J}^{-T}(\boldsymbol{\theta})\boldsymbol{\tau} + \boldsymbol{F}, \quad (2)$$

where $\boldsymbol{\theta}$ is the vector of generalized joint coordinates describing the pose of the manipulator, $\dot{\boldsymbol{\theta}}$ is the vector of joint velocity, $\boldsymbol{H}_x(\boldsymbol{\theta}, \dot{\boldsymbol{\theta}})$ is the Coriolis and centrifugal forces in Cartesian coordinate system, $\boldsymbol{G}_x(\boldsymbol{\theta})$ is

the gravity term, $\boldsymbol{J}(\boldsymbol{\theta})$ is the Jacobian matrix, and $\boldsymbol{\tau}$ is the joint driving torque vector. If it is assumed that the displacement of $\boldsymbol{x}$ in Equation (1) is very small and the inertia term can be ignored, then Equation (1) is simplified to a compliance model written by a first-order lag system. Accordingly, defining $\boldsymbol{X} \coloneqq \boldsymbol{x} - \boldsymbol{x}_d$ gives

$$\dot{\boldsymbol{X}} = \boldsymbol{A}\boldsymbol{X} + \boldsymbol{B}\boldsymbol{u}, \tag{3}$$

where

$$\boldsymbol{A} \coloneqq -\boldsymbol{B}_d^{-1}\boldsymbol{K}_d, \quad \boldsymbol{B} \coloneqq \boldsymbol{B}_d^{-1},$$

$$\boldsymbol{u} \coloneqq \{\boldsymbol{S}\boldsymbol{F} + (\boldsymbol{I} - \boldsymbol{S})\boldsymbol{K}_f(\boldsymbol{F} - \boldsymbol{F}_d)\}.$$

In general, the equation of state given by Equation (3) is solved as

$$\boldsymbol{X} = \boldsymbol{e}^{\boldsymbol{A}t}\boldsymbol{X}(0) + \int_0^t \boldsymbol{e}^{\boldsymbol{A}(t-\delta)}\boldsymbol{B}\boldsymbol{u}(\delta)d\delta. \tag{4}$$

In the following, we consider the form in the discrete time k using a sampling time Δt. It is assumed that $\boldsymbol{u}$, $\boldsymbol{A}$, and $\boldsymbol{B}$ are constant at $\Delta t(k-1) \le t < \Delta tk$. Defining $\boldsymbol{X}(k) = \boldsymbol{X}(t)|_{t=\Delta tk}$ leads to the following equation [8].

$$\begin{aligned}\boldsymbol{X}(k) &= \boldsymbol{e}^{\boldsymbol{A}\Delta tk}\left(\boldsymbol{X}(0) + \int_0^{\Delta tk} \boldsymbol{e}^{-\boldsymbol{A}\delta}\boldsymbol{B}\boldsymbol{u}(\delta)d\delta\right) \\ &= \boldsymbol{e}^{\boldsymbol{A}\Delta t}\boldsymbol{X}(k-1) + \boldsymbol{e}^{\boldsymbol{A}\Delta tk}\int_{\Delta t(k-1)}^{\Delta tk} \boldsymbol{e}^{-\boldsymbol{A}\delta}d\delta\,\boldsymbol{B}\boldsymbol{u}(k) \\ &= \boldsymbol{e}^{\boldsymbol{A}\Delta t}\boldsymbol{X}(k-1) + \left(\boldsymbol{e}^{\boldsymbol{A}\Delta t} - \boldsymbol{I}\right)\boldsymbol{A}^{-1}\boldsymbol{B}\boldsymbol{u}(k). \end{aligned} \tag{5}$$

By remembering $\boldsymbol{X}(k) = \boldsymbol{x}(k) - \boldsymbol{x}_d(k)$, the recursive equation of position command in the Cartesian space can be derived as

$$\begin{aligned}\boldsymbol{x}(k) = \boldsymbol{x}_d(k) &+ \boldsymbol{e}^{-(\boldsymbol{B}_d^{-1}\boldsymbol{K}_d)\Delta t}\{\boldsymbol{x}(k-1) - \boldsymbol{x}_d(k-1)\} \\ &- \{\boldsymbol{e}^{-(\boldsymbol{B}_d^{-1}\boldsymbol{K}_d)\Delta t} - \boldsymbol{I}\}\boldsymbol{K}_d^{-1}\{\boldsymbol{S}\boldsymbol{F} + (\boldsymbol{I} - \boldsymbol{S})\boldsymbol{K}_f(\boldsymbol{F} - \boldsymbol{F}_d)\}. \end{aligned} \tag{6}$$

Here, if it is assumed that $\boldsymbol{J}$ is also a constant matrix at $\Delta t(k-1) \le t < \Delta tk$, then a relation of $\boldsymbol{x}(k) = \boldsymbol{J}\boldsymbol{\theta}(k)$ is used. Thus, premultiplying both sides of Equation (6) by $\boldsymbol{J}^{-1}$, the recursive equation of position command in the joint space is obtained as

$$\boldsymbol{\theta}(k) = \boldsymbol{\theta}_d(k) + \boldsymbol{J}^{-1}(\boldsymbol{\theta})\boldsymbol{e}^{(\boldsymbol{B}_d^{-1}\boldsymbol{K}_d)\Delta t}\boldsymbol{J}(\boldsymbol{\theta})\{\boldsymbol{\theta}(k-1) - \boldsymbol{\theta}_d(k-1)\}$$

$$- \boldsymbol{J}^{-1}(\boldsymbol{\theta})\left\{\boldsymbol{e}^{(\boldsymbol{B}_d^{-1}\boldsymbol{K}_d)\Delta t} - \boldsymbol{I}\right\}\boldsymbol{K}_d^{-1}\{\boldsymbol{S}\boldsymbol{F} + (\boldsymbol{I} - \boldsymbol{S})\boldsymbol{K}_f(\boldsymbol{F} - \boldsymbol{F}_d)\}. \quad (7)$$

Note that the desired trajectory, which has been calculated in advance are given to $\boldsymbol{x}_d(k)$ and $\boldsymbol{\theta}_d(k)$ in the compliance control mode, whereas, the balanced position is substituted into them in the force control mode.

2.2. Transformation from position-based command to torque-based command

To simulate the position-based CMFFC, the manipulated value of position calculated from Equation (6) or Equation (7) has to be transformed to the joint driving torque for a manipulator. Therefore, a transformation technique is proposed, in which the manipulated value of position is given as the reference value of the servo system such as a resolved acceleration controller written by

$$\boldsymbol{\tau} = \boldsymbol{M}(\boldsymbol{\theta})\boldsymbol{J}^{-1}(\boldsymbol{\theta})\{\ddot{\boldsymbol{x}}_d + \boldsymbol{K}_v(\dot{\boldsymbol{x}}_d - \dot{\boldsymbol{x}}) + \boldsymbol{K}_p(\boldsymbol{x}_d - \boldsymbol{x}) - \dot{\boldsymbol{J}}(\boldsymbol{\theta})\dot{\boldsymbol{\theta}}\} + \boldsymbol{H}(\boldsymbol{\theta}, \dot{\boldsymbol{\theta}}) + \boldsymbol{G}(\boldsymbol{\theta}), \quad (8)$$

where $\ddot{\boldsymbol{x}}_d$, $\dot{\boldsymbol{x}}_d$, and $\boldsymbol{x}_d$ are the reference values of acceleration, velocity, and position, respectively. $\boldsymbol{K}_v = \mathrm{diag}(K_{v1}, \ldots, K_{v6})$ and $\boldsymbol{K}_p = \mathrm{diag}(K_{p1}, \ldots, K_{p6})$ are the feedback gains of velocity and position, respectively. The resolved acceleration controller can yield joint driving torques to independently control each joint.

First of all, by using a discrete time, the velocity and acceleration are generated as follows

$$\dot{\boldsymbol{x}}(\Delta tk) \simeq \{\boldsymbol{x}(\Delta tk) - \boldsymbol{x}(\Delta t(k-1))\} / \Delta t, \tag{9}$$

$$\ddot{\boldsymbol{x}}(\Delta tk) \simeq \{\dot{\boldsymbol{x}}(\Delta tk) - \dot{\boldsymbol{x}}(\Delta t(k-1))\} / \Delta t. \tag{10}$$

For example, in the case that the resolved acceleration control law is used in a manipulator's servo system, if $\boldsymbol{x}(\Delta tk)$, $\dot{\boldsymbol{x}}(\Delta tk)$, $\ddot{\boldsymbol{x}}(\Delta tk)$ generated from Equations (6), (9), and (10) are, respectively, given to the reference values $\boldsymbol{x}_d$, $\dot{\boldsymbol{x}}_d$, $\ddot{\boldsymbol{x}}_d$ in Equation (8), then the joint torque can be generated using the control rule itself given by Equation (8). The block diagram of this transformation is illustrated in Figure 2. It is also possible to generate the joint torque vector by giving $\boldsymbol{\theta}(\Delta tk)$, $\dot{\boldsymbol{\theta}}(\Delta tk)$, $\ddot{\boldsymbol{\theta}}(\Delta tk)$ to the reference value for the computed torque control law, which is another representative servo system. As can be seen, the proposed transformation method allows us not only to implement the position-based CMFFC in a computer simulation, but also to apply it to an actual industrial robot, whose inner servo system is technically opened.

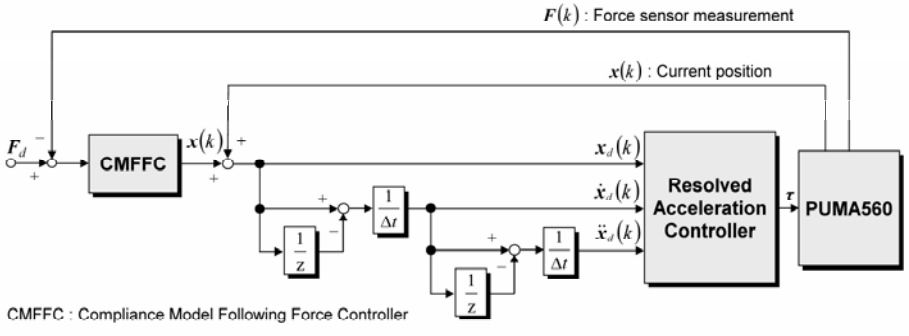

Figure 2. Transformation from position command $\boldsymbol{x}(k)$ in Cartesian space to torque command $\boldsymbol{\tau}(k)$.

3. Tuning of Desired Damping

After this section, in order to examine how the consideration of critical damping has an effect on the force control performance, we compare the conventional torque-based HCC with the proposed CMFFC by using some computer simulations. A tuning method of desired damping is considered by using the critically damped condition of force control system.

3.1. Critically damped condition of joint torque-based HCC

The control law of the joint torque-based HCC [5] is given by

$$\boldsymbol{\tau} = \boldsymbol{J}^T(\theta)\left[\boldsymbol{B}_d(\dot{\boldsymbol{x}}_d - \dot{\boldsymbol{x}}) + \boldsymbol{S}\boldsymbol{K}_d(\boldsymbol{x}_d - \boldsymbol{x}) + (\boldsymbol{I} - \boldsymbol{S})\{\boldsymbol{K}_f(\boldsymbol{F} - \boldsymbol{F}_d) - \boldsymbol{F}\}\right] + \boldsymbol{H}(\theta, \dot{\theta}) - \boldsymbol{M}(\theta)\boldsymbol{J}^{-1}(\theta)\dot{\boldsymbol{J}}(\theta)\dot{\theta} + \boldsymbol{G}(\theta). \quad (11)$$

In the case of $\boldsymbol{S} = \boldsymbol{I}$, Equation (11) is used to construct a closed-loop system of the position and velocity. On the other hand, in the case of $\boldsymbol{S} = \boldsymbol{0}$, Equation (11) is applied to form a closed-loop system of the velocity and force.

We here propose a systematic method, which can easily calculate the desired damping considering the critically damped condition of force control system, without any trial and error. Figure 3 shows the contact situation, in which the force acting on the end-effector is caused by the collision to an object and is assumed to be modelled by

$$\boldsymbol{F} = -\boldsymbol{B}_m\dot{\boldsymbol{x}} - \boldsymbol{K}_m(\boldsymbol{x} - \boldsymbol{x}_m), \quad \boldsymbol{x} \geq \boldsymbol{x}_m, \quad (12)$$

where $\boldsymbol{B}_m$ and $\boldsymbol{K}_m$ are the viscosity and stiffness coefficients of the object assumed to be positive definite diagonal matrices, and $\boldsymbol{x}_m$ is the position vector of the object. If the contact force is given by Equation (12), the desired response in the joint torque-based HCC can be rewritten as

$$\boldsymbol{M}_x(\theta)\ddot{\boldsymbol{x}} + \boldsymbol{B}_d(\dot{\boldsymbol{x}} - \dot{\boldsymbol{x}}_d) + \boldsymbol{S}\boldsymbol{K}_d(\boldsymbol{x} - \boldsymbol{x}_d) = \boldsymbol{S}\{-\boldsymbol{B}_m\dot{\boldsymbol{x}} - \boldsymbol{K}_m(\boldsymbol{x} - \boldsymbol{x}_m)\} + (\boldsymbol{I} - \boldsymbol{S})\boldsymbol{K}_f\{-\boldsymbol{B}_m\dot{\boldsymbol{x}} - \boldsymbol{K}_m(\boldsymbol{x} - \boldsymbol{x}_m) - \boldsymbol{F}_d\}. \quad (13)$$

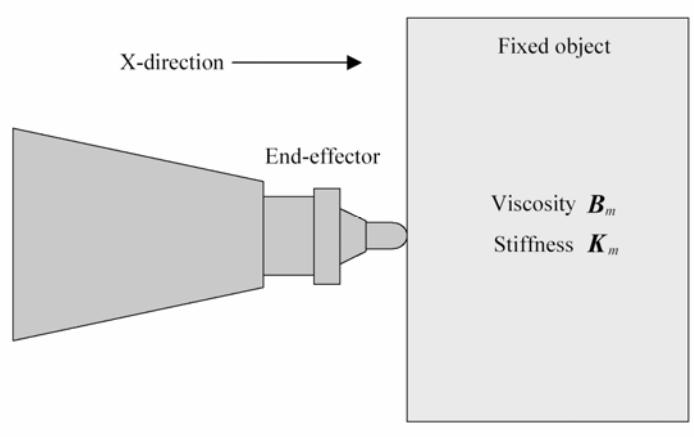

Figure 3. Force control scene between an end-effector and a fixed object.

Since each of coefficient matrices $\boldsymbol{B}_d$, $\boldsymbol{K}_d$, $\boldsymbol{B}_m$, $\boldsymbol{K}_m$, and $\boldsymbol{K}_f$ is diagonal, if the diagonal elements M_{xi} of $\boldsymbol{M}_x$ are sufficiently larger than non-diagonal elements, each differential equation of Equation (13) is nearly decoupled. In this case, the critically damped condition of Equation (13) is obtained by

$$\left[B_{di} + \{S_i B_{mi} + (1 - S_i) K_{fi} B_{mi}\}\right]^2 = 4 M_{xi} \left[S_i K_{di} + \{S_i K_{mi} + (1 - S_i) K_{fi} K_{mi}\}\right], \tag{14}$$

where B_{di}, K_{di}, B_{mi}, K_{mi}, and K_{fi} denote the i-th diagonal elements of $\boldsymbol{B}_d$, $\boldsymbol{K}_d$, $\boldsymbol{B}_m$, $\boldsymbol{K}_m$, and $\boldsymbol{K}_f$, respectively. Therefore, the solution $\widetilde{B}_{di}$ of Equation (14) can be calculated by

$$\widetilde{B}_{di} = 2\sqrt{\{\boldsymbol{J}^{-T}(\boldsymbol{\theta})\boldsymbol{M}(\boldsymbol{\theta})\boldsymbol{J}^{-1}(\boldsymbol{\theta})\}_i \left[S_i K_{di} + \{S_i K_{mi} + (1 - S_i) K_{fi} K_{mi}\}\right]} - \{S_i B_{mi} + (1 - S_i) K_{fi} B_{mi}\}, \tag{15}$$

where $\boldsymbol{J}^{-T}(\boldsymbol{\theta})\boldsymbol{M}(\boldsymbol{\theta})\boldsymbol{J}^{-1}(\boldsymbol{\theta}) = \boldsymbol{M}_x(\boldsymbol{\theta})$, and $\{\boldsymbol{J}^{-T}(\boldsymbol{\theta})\boldsymbol{M}(\boldsymbol{\theta})\boldsymbol{J}^{-1}(\boldsymbol{\theta})\}_i$ is the i-th diagonal element of $(\cdot)$. The inertia matrix $\boldsymbol{M}(\boldsymbol{\theta})$ and Jacobian $\boldsymbol{J}(\boldsymbol{\theta})$ in the joint space are variable and nonlinear with respect to the variation of a manipulator pose. That is to say, in order to control the manipulator

with critical damping, irrespective of the variation of the pose, $\boldsymbol{B}_d$ should be varied according to Equation (15). An improved control law using Equation (15) is rewritten as

$$\boldsymbol{\tau} = \boldsymbol{J}^T(\boldsymbol{\theta})[\tilde{\boldsymbol{B}}_d(\dot{\boldsymbol{x}}_d - \dot{\boldsymbol{x}})\boldsymbol{S}\boldsymbol{K}_d(\boldsymbol{x}_d - \boldsymbol{x}) + (\boldsymbol{I} - \boldsymbol{S})\{\boldsymbol{K}_f(\boldsymbol{F} - \boldsymbol{F}_d) - \boldsymbol{F}\}] + \boldsymbol{H}(\boldsymbol{\theta}, \dot{\boldsymbol{\theta}}) - \boldsymbol{M}(\boldsymbol{\theta})\boldsymbol{J}^{-1}(\boldsymbol{\theta})\dot{\boldsymbol{J}}(\boldsymbol{\theta})\dot{\boldsymbol{\theta}} + \boldsymbol{G}(\boldsymbol{\theta}). \quad (16)$$

3.2. Critically damped condition of CMFFC

For the CMFFC in the Cartesian coordinate system, the manipulated variable is given by Equation (6). For example, after the end-effector contacts to a fixed object, setting $\boldsymbol{S} = \boldsymbol{I}$ yields a compliance control mode in all directions, also setting $\boldsymbol{S} = \boldsymbol{0}$ gives a force control mode in all directions to keep contact with the object with a constant force $\boldsymbol{F}_d$. The compliance control absorbs the shock caused by the collision, and the force control achieves the desired force convergence at last.

From Equation (1), the dynamic equation for the CMFFC is written by

$$\boldsymbol{M}_x(\boldsymbol{\theta})\ddot{\boldsymbol{x}} + \boldsymbol{B}_d(\dot{\boldsymbol{x}} - \dot{\boldsymbol{x}}_d) + \boldsymbol{K}_d(\boldsymbol{x} - \boldsymbol{x}_d) = \boldsymbol{S}\{-\boldsymbol{B}_m\dot{\boldsymbol{x}} - \boldsymbol{K}_m(\boldsymbol{x} - \boldsymbol{x}_m)\} + (\boldsymbol{I} - \boldsymbol{S})\boldsymbol{K}_f\{-\boldsymbol{B}_m\dot{\boldsymbol{x}} - \boldsymbol{K}_m(\boldsymbol{x} - \boldsymbol{x}_m) - \boldsymbol{F}_d\}. \quad (17)$$

In the same way as HCC, considering the critically damped condition of Equation (17) gives

$$\tilde{B}_{di} = 2\sqrt{\{\boldsymbol{J}^{-T}(\boldsymbol{\theta})\boldsymbol{M}(\boldsymbol{\theta})\boldsymbol{J}^{-1}(\boldsymbol{\theta})\}_i\left[K_{di} + \{S_iK_{mi} + (1 - S_i)K_{fi}K_{mi}\}\right]} - \{S_iB_{mi} + (1 - S_i)K_{fi}B_{mi}\}. \quad (18)$$

The manipulated variable of position with $\tilde{B}_{di}$ calculated from Equation (18) is rewritten as

$$\boldsymbol{x}(k) = \boldsymbol{x}_d(k) + \boldsymbol{e}^{-(\tilde{\boldsymbol{B}}_d^{-1}\boldsymbol{K}_d)\Delta t}\{\boldsymbol{x}(k-1) - \boldsymbol{x}_d(k-1)\} - \{\boldsymbol{e}^{-(\tilde{\boldsymbol{B}}_d^{-1}\boldsymbol{K}_d)\Delta t} - \boldsymbol{I}\}\{\boldsymbol{S}\boldsymbol{F} + (\boldsymbol{I} - \boldsymbol{S})\boldsymbol{K}_f(\boldsymbol{F} - \boldsymbol{F}_d)\}. \quad (19)$$

4. Force Control Simulation

Figure 3 shows the experimental scene of force control, in which the end-effector contacts to an object from the minus direction of x-axis. In this case, B_{mx} and K_{mx} are assumed as 10 [Ns/m] and 1000 [N/m], respectively. It is tried to control the contact force F_x in the direction of x-axis to converge to the reference value $F_{dx} = 1$ [N]. It is assumed that the end-effector approaches from the point at the distance of 0.02 [m] to the object with a velocity of 0.0184 [m/s], and keeps contact with the object. The simulation is carried out by using the Runge-Kutta-Gill method with the kinematic and dynamic parameters of PUMA560 manipulator [1, 2]. Simulation time and sampling width are set to 5 [s] and 10 [ms], respectively.

4.1. In the case of joint torque-based HCC

Equations (11) and (16) were used in the simulation. A trajectory tracking control was implemented, until the end-effector contacted to the object, in which the desired trajectory prepared in advance was given to the desired position. The desired trajectory was calculated with 4-1-4 order polynomial equation to reach a low velocity of 0.0184 [m/s] for one second from a standstill situation. After contacting to the object, the balanced position $x_{mx} - F_{dx}K_{mx}^{-1}$ was given to the desired position $\boldsymbol{x}_d$, and then the force control mode was carried out only in x-direction.

4.1.1. Constant desired damping coefficient

Figure 4 shows the force control result in case of using Equation (11) as a control law, where B_{dx} and K_{dx} are set to 20 [Ns/m] and 400 [N/m], respectively. As can be seen, undesirable oscillations are observed just after contacting the object.

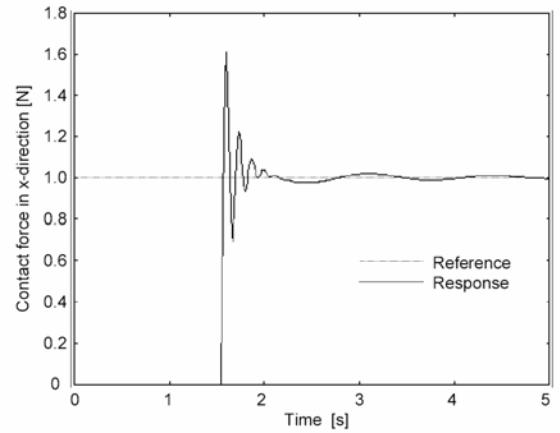

Figure 4. Contact force in *x*-direction with a constant desired damping.

4.1.2. Time-varying desired damping coefficient

Figure 5 shows the force control result in case of using Equation (16), in which the desired damping in the direction of *x*-axis is varied according to Equation (15). Figure 6 shows the variation of $\widetilde{B}_{dx}$ in the direction of *x*-axis after the contact motion. It is observed that the oscillations just after the contact motion decreases satisfactorily.

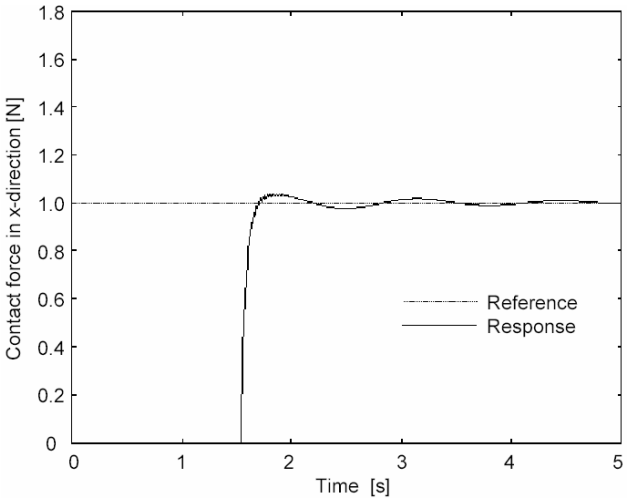

Figure 5. Contact force in *x*-direction with time-varying desired damping.

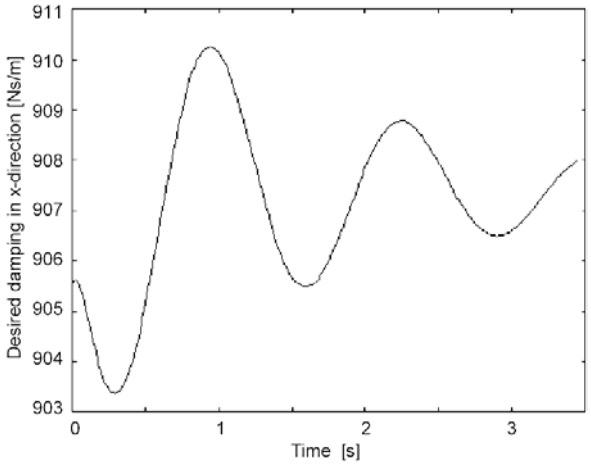

Figure 6. Time-varying desired damping in *x*-direction after the contact motion.

4.2. In the case of CMFFC

Next, the force control performance of CMFFC was examined through the same simulation as described in the previous subsection. In this case, Equations (6) and (19) were compared. The same desired trajectory as in evaluating the joint torque-based HCC was given to $x_{dx}(k)$ both in the trajectory tracking control mode before the contact motion and in compliance control mode after the contact motion. After contacting to the object, the compliance control mode with setting $S_x = 1$ absorbed the shock until the magnitude of the contact force got over 80% of the desired one, then the controller was switched to the force control mode by setting $S_x = 0$. In the force control mode, the balanced position was given to the *x*-directional desired position $x_{dx}(k)$.

4.2.1. Constant desired damping coefficient

Figure 7 shows the force control result in case of using Equation (6) as a control law, where B_{dx} and K_{dx} are similarly set to 20 [Ns/m] and 400 [N/m], respectively. As can be seen, large oscillations and a non-contact situation are observed just after contacting the object.

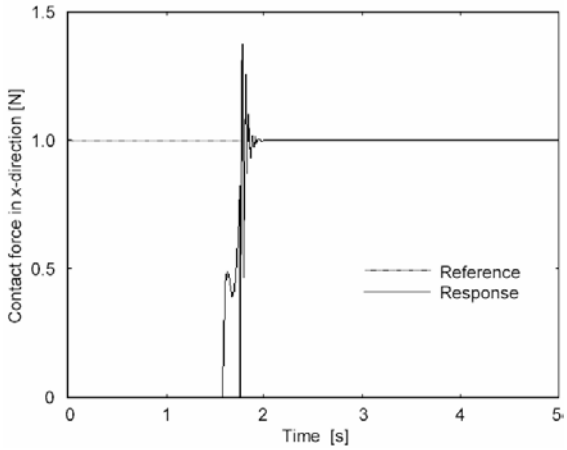

Figure 7. Contact force in *x*-direction with a constant desired damping.

4.2.2. Time-varying desired damping coefficient

On the other hand, Figure 8 shows the force control result, in which the desired damping $\widetilde{B}_{dx}$ in the direction of *x*-axis was varied with the critical damping given by Equation (18) according to the slight variation of the manipulator pose. Figure 9 shows the variation of $\widetilde{B}_{dx}$ in the force control mode. It is recognized that, the response is successfully improved without overshoots and oscillations.

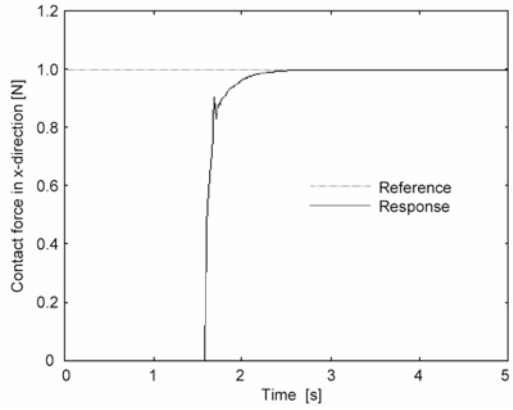

Figure 8. Contact force in *x*-direction with time-varying desired damping.

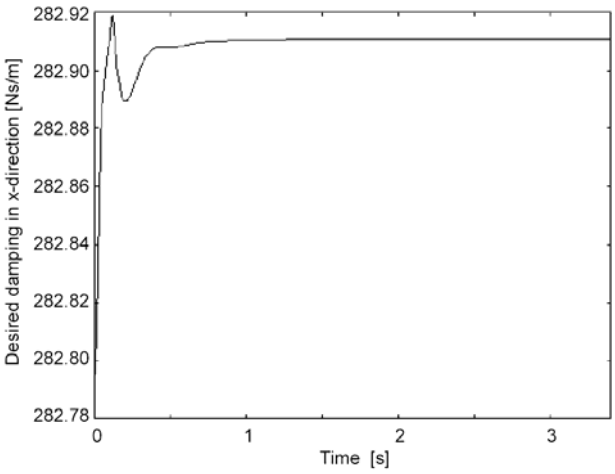

Figure 9. Time-varying desired damping in x-direction after the contact motion.

4.3. Discussions

By using the joint torque-based HCC and the position-based CMFFC, the end-effector was made to keep contact with an object, whose physical parameters are known, and to converge to a desired contact force. In the case of joint torque-based HCC, it is found from Figure 4 that, if B_{dx} is constant regardless of the variation of the manipulator pose, the overshoots and oscillations appear just after the contact motion, and later slack oscillations remain around the reference value. Also, Figure 5 shows that, if B_{dx} changes considering the critically damped condition with the known physical parameters of the object, then the response just in the contact motion is improved, but there still remain the slack oscillations similar to Figure 4.

On the other hand, in the case of the position-based CMFFC, it is confirmed from Figure 7 that, if B_{dx} is constant regardless of the variation of the manipulator pose, the overshoots and oscillations with different characteristics from the HCC appear just after the contact motion, but later the contact force converges to the reference value. Figure 8 shows that, if B_{dx} changes with the critically damped condition,

the desirable response without overshoots and oscillations can be obtained after the contact motion.

5. Conclusions

In this paper, we have proposed a position-based CMFFC that can generate joint driving torque by means of giving the manipulated value of position to technically opened inner servo system such as a resolved acceleration controller. The proposed method has allowed us not only to simulate the position-based CMFFC on MATLAB system, but also to apply the force controller to an actual industrial robot, whose servo structure is opened to technical users.

As for the tuning of control parameters, there existed a problem that a considerable amount of time was needed, i.e., the desired damping was tuned for each task by repeating simulations of trial and error in spite of known environments [5]. In order to overcome this problem, we have proposed an effective tuning method that can systematically calculate the desired damping according to the variation of manipulator pose. From the fact that, the inertia term and Jacobian change nonlinearly caused by the variation of the manipulator pose, the desired damping can be varied considering the critically damped condition in force control system. The force control performances of the joint torque-based HCC and the position-based CMFFC were examined through making the end-effector of a PUMA560 manipulator contact to an object. Consequently, the tuning method has been able to improve the performance of the force control. It will be able to be applied for the tasks like grinding and polishing, which have to be hand-worked with compliant force so as not to damage an object.

References

[1] P. Corke, A robotics toolbox for MATLAB, IEEE Robotics & Automation Magazine 3(1) (1996), 24-32.

[2] P. Corke, MATLAB Toolboxes: robotics and vision for students and teachers, IEEE Robotics & Automation Magazine 14(4) (2007), 16-17.

[3] J. J. Craig, Introduction to ROBOTICS-Mechanics and Control Second Edition, Addison Wesley Publishing Co., 1989.

[4] N. Hogan, Impedance control: An approach to manipulation: Part I-Part III, Trans. ASME J. Dynam. Syst., Measurement and Control 107 (1985), 1-24.

[5] T. Katsuragawa, K. Ioi, N. Kubota and O. Noro, Application of hybrid compliance/force control for industrial robot, Journal of the Robotics Society of Japan 12(6) (1994), 893-898 (in Japanese).

[6] K. Kosuge, Force control of manipulators, Journal of the Robotics Society of Japan 9(6) (1991), 751-758 (in Japanese).

[7] M. H. Raibert and J. J. Craig, Hybrid position/force control of manipulators, Trans. ASME J. Dynam. Syst. Measurement and Control 102 (1981), 126-133.

[8] For example, T. Yoshikawa and J. Imura, Modern Control Theory, Syokodo Publishing Co., (1996), 22-23, (in Japanese).

■